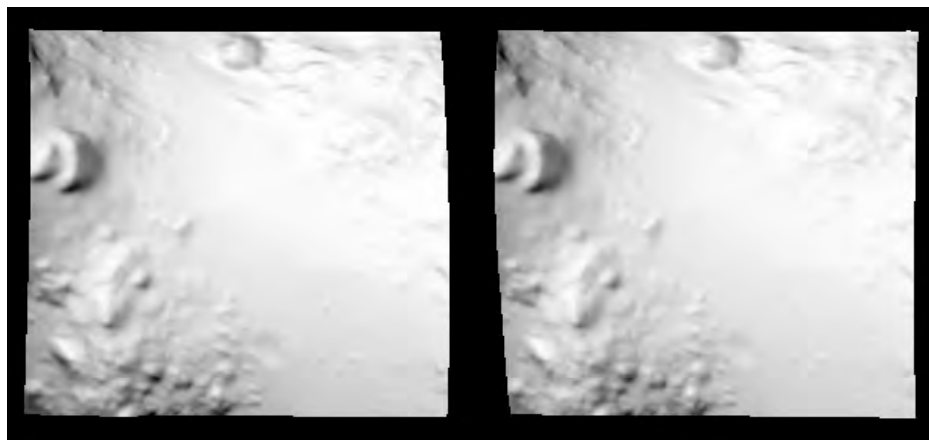


**GLOBAL TOPOGRAPHY OF ASTEROID 25143 ITOKAWA.** R. Gaskell<sup>1</sup>, J. Saito<sup>2</sup>, M. Ishiguro<sup>2</sup>, T. Kubota<sup>2</sup>, T. Hashimoto<sup>2</sup>, N. Hirata<sup>3</sup>, S. Abe<sup>3</sup>, O. Barnouin-Jha<sup>4</sup>, and D. Scheeres<sup>5</sup>. <sup>1</sup>JPL/CALTECH, Pasadena, CA, [rwg@jpl.nasa.gov](mailto:rwg@jpl.nasa.gov), <sup>2</sup>ISAS, Sagamihara, Japan, <sup>3</sup>Kobe University, Kobe, Japan, <sup>4</sup>APL/Johns Hopkins, Laurel, MD, <sup>5</sup>University of Michigan, Ann Arbor, MI

**Introduction:** A catalog of digital elevation/albedo maps covering the surface of asteroid 25143 Itokawa is being constructed by applying multi-image photogrammetry to about 600 Hayabusa AMICA science images [1]. Over 750 99x99 pixel landmark maps (L-maps) have been created so far, equivalent to more than seven million surface vectors. The maps can be combined to build global topography models (GTM), or to make high-resolution local maps, such as the stereo image of the Hayabusa landing region below.

fit of the brightness in many images. Slopes are then integrated to produce the height distribution, with external constraints coming from limbs and overlapping maps. Each map is referred to its own local coordinate system, the origin of which is the body-fixed control point.

Recently, a third procedure has been added. Once a global topography model has been constructed, the LIDAR range can be predicted for each image, and the measured range can be used to correct the spacecraft-object vector. Because Hayabusa was not an



**Figure 1:** Stereo pair showing the Hayabusa landing site region.

**Method:** The procedure [2] is divided into two parts, a geometry estimation similar to traditional multi-image stereography, and multi-image photogrammetry, which creates the L-maps. The two operations are dependent on one another, so the procedure is an iterative one.

L-maps can be identified in images under any viewing or illumination conditions and accurately positioned using digital correlation. They can also be identified on the limbs of the body in other images. Finally, overlapping maps can be aligned with each other due to their common topography. These data types allow for the least-square estimation of spacecraft position and orientation, the rotation of the body, and the body-fixed location of the map centers (control points). More than 70,000 measurements went into locating the map centers, with rms post-fit residuals of about 30 cm per degree of freedom.

The maps themselves are created by solving for slope and albedo at each map pixel in a least-square

orbital mission, Doppler data could not be used to determine the distance scale, so the LIDAR data ultimately determined the size of Itokawa.

The creation of composite maps and global topography models is accomplished in much the same way as the L-maps themselves. Because simple height averaging can contain discontinuities due to errors in the control point vectors, the slopes are averaged instead, and the slope-to-height integration is performed with a small number of averaged heights included to condition the solution.

**Discussion:** An image of the 1.57 million vector global topography model is shown in Figure 2, next to the corresponding AMICA image. The surface area is  $0.3928 \text{ km}^2$ , the volume is  $0.01752 \text{ km}^3$ , and the principal moments of inertia per unit mass are (0.00626, 0.02096, 0.02201)  $\text{km}^2$ , assuming a constant density. It is likely that these numbers will change. Currently, the LIDAR ranges average 0.5%

larger than the predicted ranges, suggesting that the final converged volume, for example, will be closer to  $0.01778 \text{ km}^3$ .

The principal z-axis differs from the axis of rotation by about 1.3 degrees in the y-direction, which may indicate a non-uniform mass distribution or a non-simple rotation. The axis of rotation is at  $90.08, -67.03$  degrees (earth equatorial) or  $266.02, -89.53$  degrees (ecliptic). This pole was determined in a simultaneous estimation with the 779 control point locations, and has a formal uncertainty of about 0.1 degrees.



Figure 2. GTM and AMICA image 2420822891

It is clear from Fig.2 that more work needs to be done, especially for features with drastic relief such as the Yoshinodai boulder at the top, and the Pencil boulder near the lower middle.

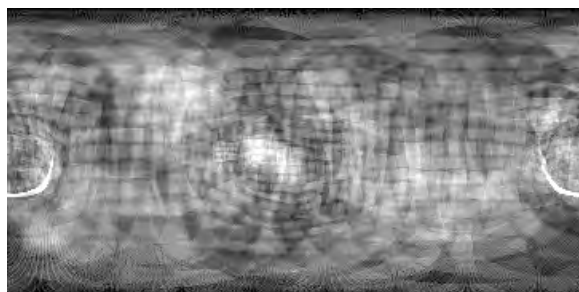


Figure 3. L-map coverage of Itokawa.

A latitude/longitude plot of the L-map coverage is shown in Figure 3. The semi-circular arc near zero longitude results from many L-maps being viewed edge on. This indicates that the surface of Itokawa, like that of Eros, cannot be represented as a function of latitude and longitude since it is multi-valued in some directions.

Eventually, the catalog of maps will be made available. The software for creating composite maps

will, also be made available, probably through NAIF, so that users can create topographic maps of selected surface regions.

#### References:

[1] Nakamura T. et al (2001) Earth Planets Space 53, 1047-1063. [2] Gaskell R, (2005) AAS\_05\_289.

#### Acknowledgement:

This work was carried out at the Institute of Space and Astronautical Science in Sagami-hara, Japan, and at the Jet Propulsion Laboratory, California Institute of Technology, under a contract with the National Aeronautics and Space Administration.